Science Advances
AAAS

advances.sciencemag.org/cgi/content/full/6/36/eaba1693/DC1

Supplementary Materials for

DSCAM regulates delamination of neurons in the developing midbrain

Nariko Arimura*, Mako Okada, Shinichiro Taya, Ken-ichi Dewa, Akiko Tsuzuki, Hirotomo Uetake, Satoshi Miyashita, Koichi Hashizume, Kazumi Shimaoka, Saki Egusa, Tomoki Nishioka, Yuchio Yanagawa, Kazuhiro Yamakawa, Yukiko U. Inoue, Takayoshi Inoue, Kozo Kaibuchi, Mikio Hoshino*

*Corresponding author. Email: n-arimur@ncnp.go.jp (N.A.); hoshino@ncnp.go.jp (M.H.)

Published 2 September 2020, *Sci. Adv.* **6**, eaba1693 (2020)
DOI: 10.1126/sciadv.aba1693

The PDF file includes:

Other Supplementary Material for this manuscript includes the following:

(available at advances.sciencemag.org/cgi/content/full/6/36/eaba1693/DC1)

Supplementary Information

Figures

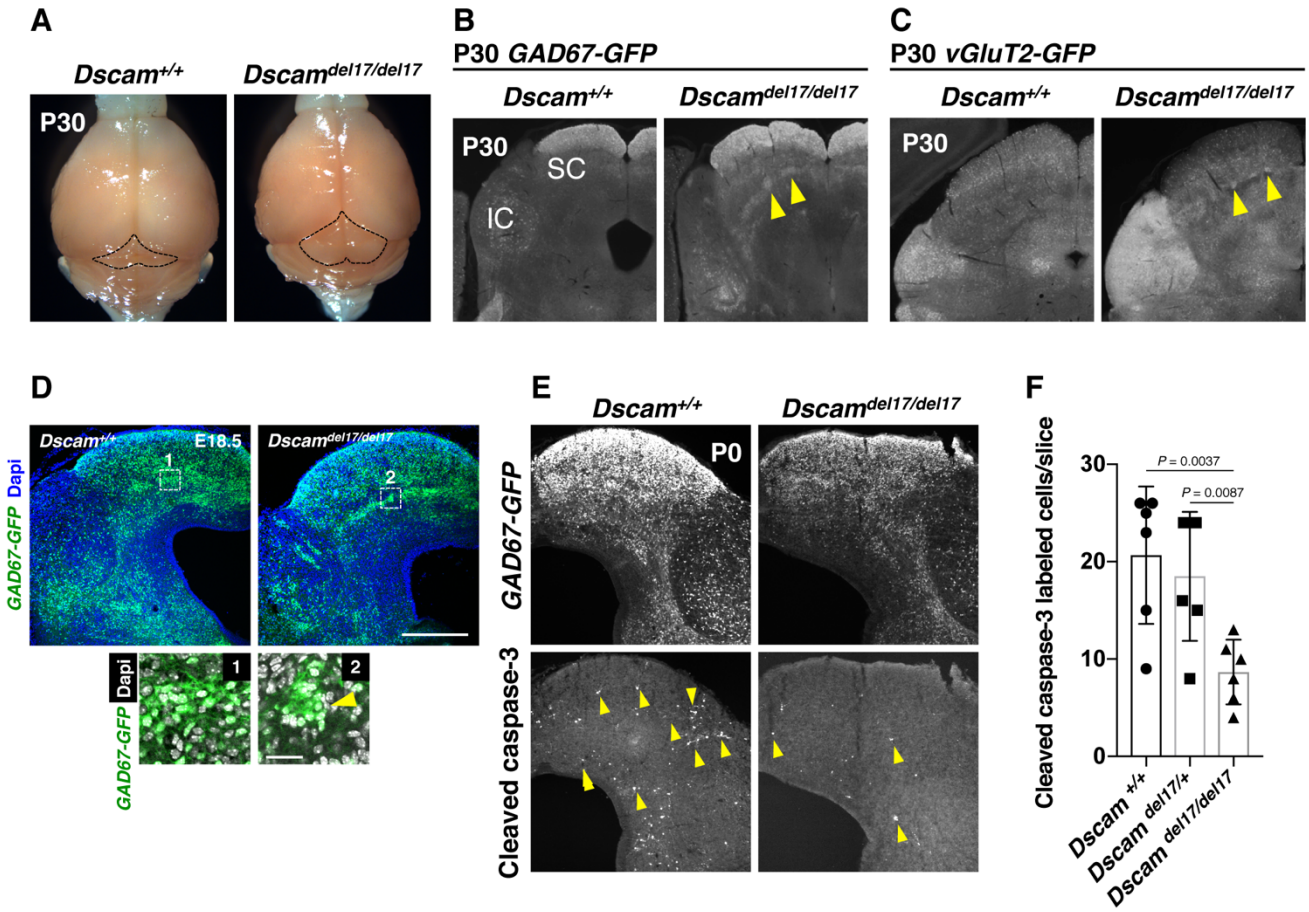

Fig. S1. Hypertrophy, cell clustering, and apoptosis inhibition in *Dscam*$^{del17/del17}$ mice. (**A**) Hypertrophy of the dorsal midbrain (dotted line) in *Dscam*$^{del17/del17}$ mice at P30. (Photo credit: N. Arimura, National Center of Neurology and Psychiatry) (**B**) Clusters of GAD67-GFP-positive cells in the superior colliculus (SC) and inferior colliculus (IC) at P30. The yellow arrowheads indicate clustering of GFP-labeled inhibitory neurons. (**C**) Cluster of vGluT2-GFP-positive cells in the SC at P30. The yellow arrowheads indicate clustering of GFP-labeled excitatory neurons. (**D**) Inhibitory neuron clusters observed during the last stage of midbrain development E18.5 in GAD-GFP; *Dscam*$^{del17/del17}$ mice. Scale bar: 400 μm. Numbered areas surrounded by dotted lines are shown at a higher magnification at the bottom. The yellow arrowhead indicates clustering of GFP-labeled inhibitory neurons. Scale bar: 30 μm. (**E**) Immunohistochemical analyses using P0 *Dscam*$^{+/+}$ and *Dscam*$^{del17/del17}$ mice.

Several cleaved caspase-3-positive cells were observed throughout the SC and IC areas in control brains (*Dscam*$^{+/+}$), but only some of these cells were detected in *Dscam*$^{del17/del17}$ brains at P0. The yellow arrowheads indicate cleaved caspase-3-positive cells. (**F**) Analysis of the number of cleaved caspase-3-positive delaminating neurons in each control or mutant midbrain at P0 (*Dscam*$^{+/+}$, n = 6; *Dscam*$^{del17/+}$, n = 5; *Dscam*$^{del17/del17}$, n = 6). Data are presented as the mean ± SEM; unpaired two-tailed *t*-test.

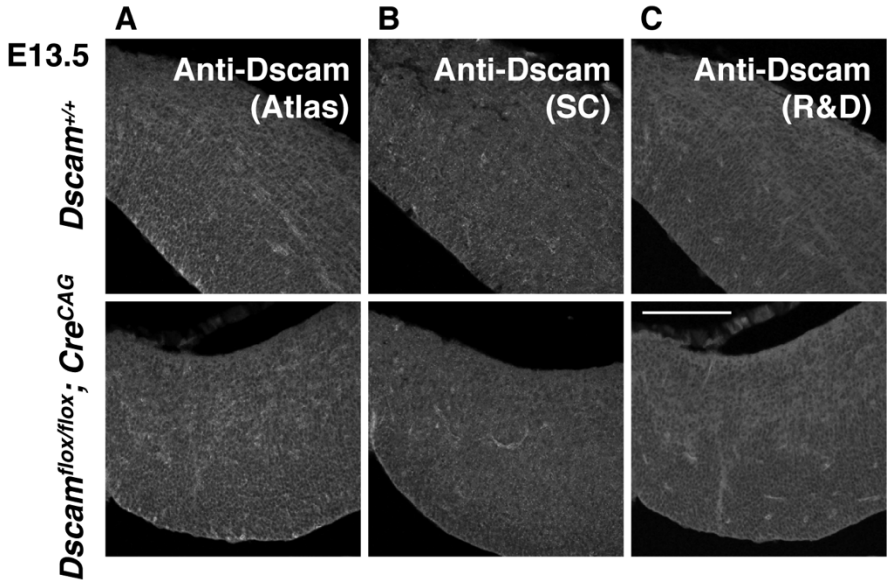

Fig. S2. Immunohistochemical analyses using three anti-DSCAM antibodies in coronal sections of the dorsal midbrain. Immunohistochemical analyses using coronal sections of control (*Dscam*$^{+/+}$) or *Dscam* knockout (KO) mice (*Dscam*$^{flox/flox}$*; Cre*^{CAG}) at E13.5. Three antibodies were used against DSCAM. (**A**) Anti-DSCAM antibody produced in rabbit (HPA019324; Atlas antibodies). (**B**) Anti-DSCAM antibody produced in rabbit (N-16; sc-79437; Santa Cruz Biotechnology [SC]). (**C**) Anti-DSCAM antibody produced in goat (AF3666; R&D Systems). Using all three antibodies, several immunohistochemical conditions, including different antibody dilutions (1:100–1:5000), blocking buffers (normal donkey serum, BSA, or skim milk), fixation conditions (4% or 2% PFA), and target retrieval method (boiling the sections for 20 min in Target Retrieval Solution pH 6 [DAKO]), were tested. However, we were unable to obtain any distinct signals to distinguish control and *Dscam* KO mice, suggesting that other antigens similar to DSCAM may be expressed in the midbrain. The staining conditions for the sections for which images are presented in A–C are as follows: 1:500 antibody dilution, normal donkey serum as blocking buffer, and 4% PFA fixation without target retrieval. Scale bar: 100 μm.

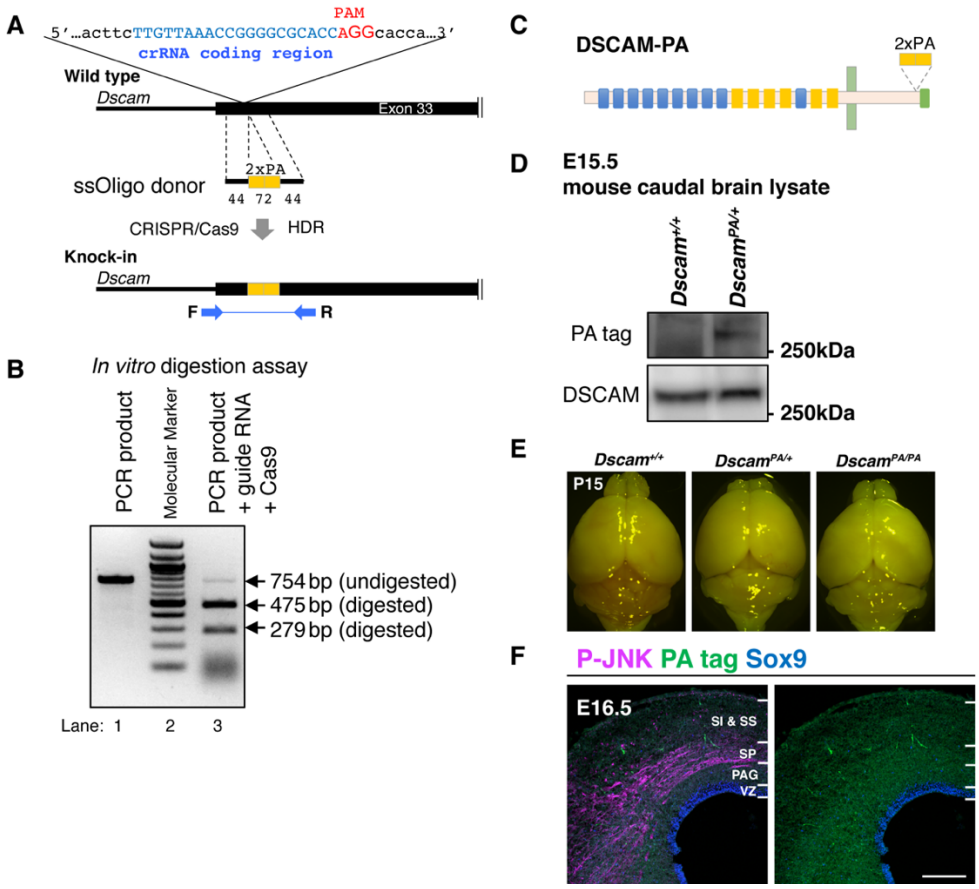

Fig. S3. Generation of PA tag knock-in mice by the CRISPR/Cas system. (**A**) Targeting strategy for the generation of *Dscam-PA tag* KI mice. We designed the guide sequence targeting the cytoplasmic region of mouse *Dscam.* A single strand oligo donor was generated encoding the 72 bp tandem PA (2xPA) tag sequence flanked by 44 bp homology arms on both sides. Genotyping of the mouse tail genome was performed using forward (F) and reverse (R) primers. (**B**) *In vitro* digestion assay to verify cleavage activity of the crRNA designed in (**A**). The targeted *Dscam* PCR product (lane 1) was incubated with chemically synthesized guide RNA (Dscam-crRNA and tracer RNA) and Cas9 protein at 37°C for 60 min, following which it was loaded in lane 3. This PCR product was cleaved by chemically synthesized crRNA/tracrRNA combined with Cas9 protein with efficiencies of over 90%. (**C**) Diagram of the domain structure of the DSCAM-PA protein. (**D**) Confirmation of DSCAM-PA protein expression using caudal brain lysates by western blotting using anti-PA tag and anti-DSCAM

antibodies. (**E**) Overall brain structure of P15 mice for the indicated genotypes. Brains of mice heterozygous and homozygous for Dscam-PA are indistinguishable from those of control mice. (Photo credit: N. Arimura, National Center of Neurology and Psychiatry) (**F**) Confirmation of the localization of the DSCAM-PA protein by anti-phospho JNK (P-JNK) and anti-Sox9 antibodies in E16.5 *Dscam*$^{PA/+}$ mice. Immunohistochemical analyses revealed that DSCAM-PA (green) mainly accumulated in the PAG (inner area, weak staining with phospho-JNK [magenta]) and SP (middle area, strong staining with phosphor-JNK) areas. The VZ was verified using Sox9 (blue). SI, strata intermedium; SS, strata superficiale; SP, strata profundum; PAG, periaqueductal gray; VZ, ventricular zone. Scale bar: 100 μm.

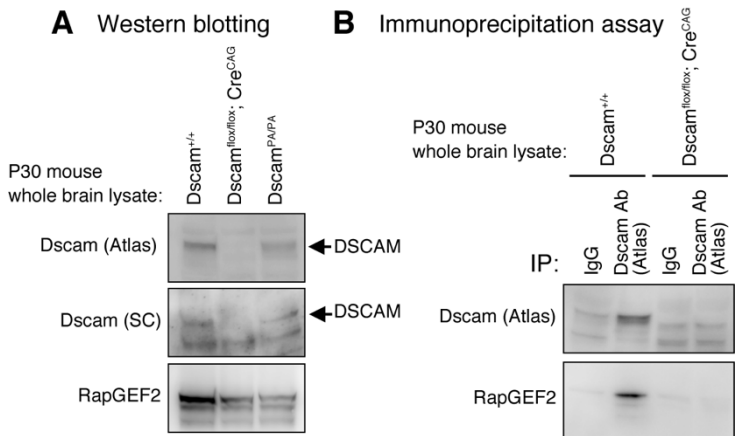

Fig. S4. Validation of anti-DSCAM antibodies (Atlas and SC) via western blotting and immunoprecipitation. (**A**) Western blot analysis was performed using P30 whole brain lysates of control (*Dscam*$^{+/+}$), *Dscam* knockout (KO) (*Dscam*$^{flox/flox}$*; Cre*^{CAG}), and *Dscam*$^{PA/PA}$ mice. Anti-DSCAM antibodies (HPA019324; Atlas antibodies, and N-16; sc-79437; Santa Cruz Biotechnology [SC]) bound to full-length DSCAM in the brain lysates of control but not those of *Dscam* KO mice, confirming the specificity of these antibodies for DSCAM. These antibodies also detected DSCAM *Dscam*$^{PA/PA}$ in mouse brains, suggesting that DSCAM-PA was appropriately expressed by the knock-in allele. (**B**) An immunoprecipitation assay was performed using an anti-DSCAM antibody (Atlas) and the indicated brain lysates. The anti-DSCAM antibody (Atlas) specifically and efficiently immunoprecipitated full-length DSCAM. Using this antibody (Atlas), RapGEF2 efficiently coimmunoprecipitated with DSCAM.

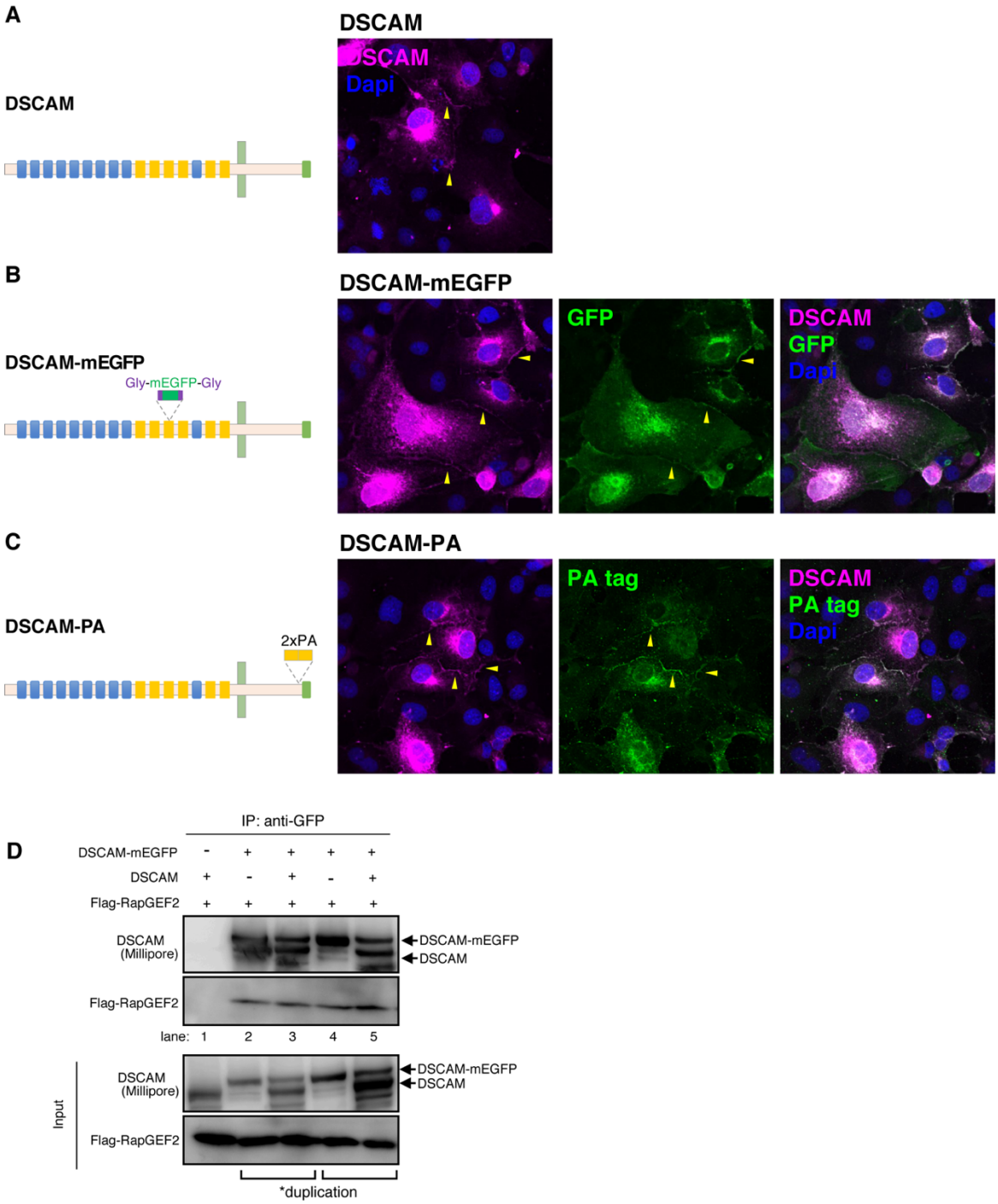

Fig. S5. Validation of Dscam constructs in cultured cells. (**A-C**) Distribution of DSCAM-mEGFP and DSCAM-PA in COS7 cells. COS7 cells were electroporated with the indicated expression plasmids. Two days following electroporation, DSCAM was detected with an anti-DSCAM antibody (SIGMA). GFP (**B**) and PA-tag (**C**) were detected using specific antibodies. The distributions of DSCAM, DSCAM-mEGFP, and DSCAM-PA were similar and indistinguishable from one another. (**D**) Immunoprecipitation assay to validate DSCAM-

mEGFP expression, using COS7 cells transfected with indicated expression vectors (non-tagged DSCAM, DSCAM-mEGFP, and Flag-RapGEF2). Non-tagged DSCAM coimmunoprecipitated with DSCAM-mEGFP and Flag-RapGEF2 using anti-GFP antibody, suggesting that DSCAM-mEGFP can bind to non-tagged DSCAM and RapGEF2.

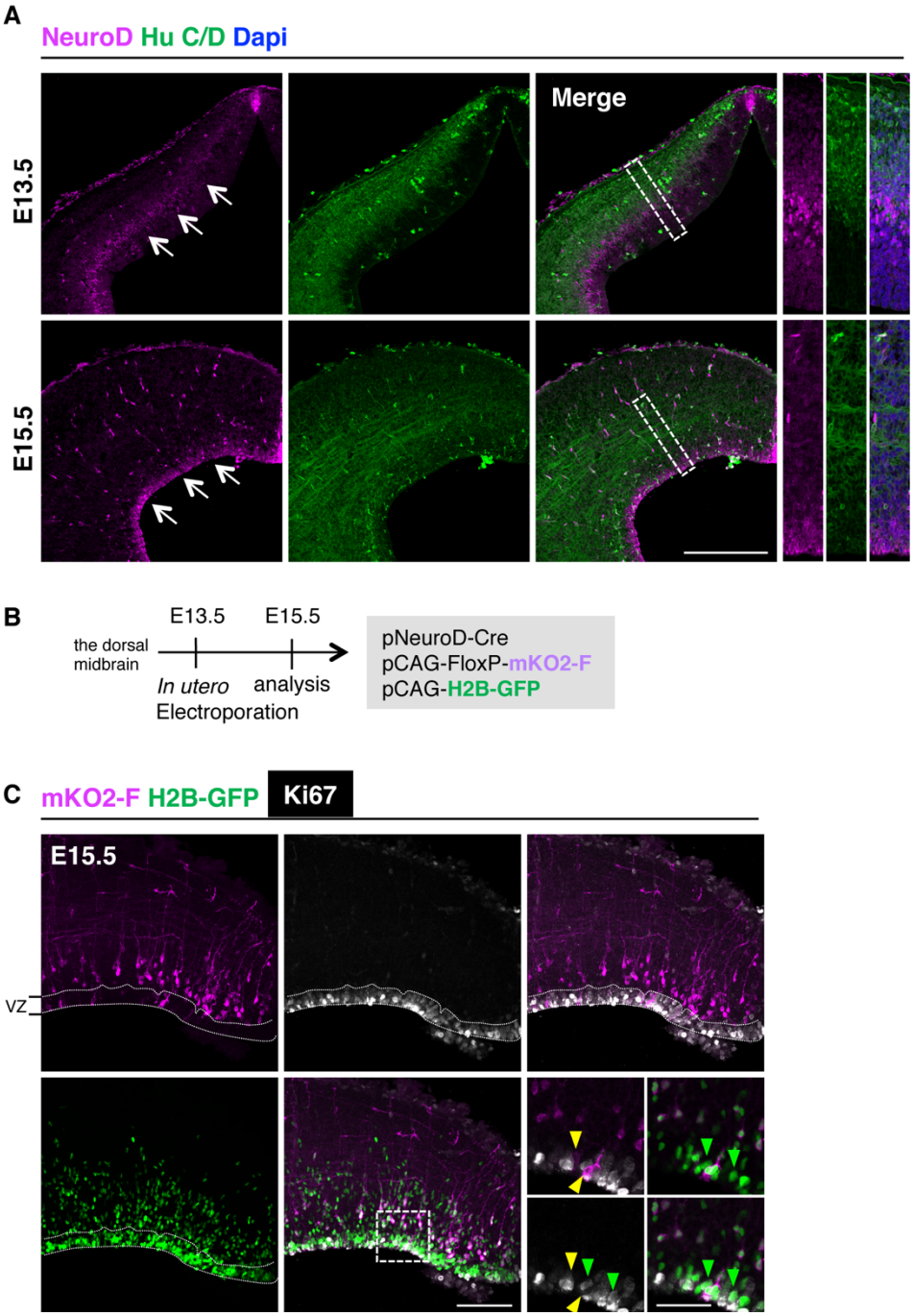

Fig. S6. Verification of endogenous NeuroD and NeuroD-promoter-driven mKO2-F expression.

(**A**) Endogenous NeuroD expression in the dorsal midbrain at E13.5 and E15.5. Upper column: endogenous NeuroD protein (magenta) is expressed at the border of the interphase of the VZ and IZ at E13.5. We previously reported that although NeuroD-positive cells did not co-express Ki67, some co-expressed Hu C/D (green), an early pan-neuronal marker, suggesting that these cells are immature post-mitotic neurons. Lower column: endogenous

NeuroD protein is weakly expressed in the thin layer near the side of a ventricle at E15.5. This is because the VZ becomes thinner during the last stage of neurogenesis in the dorsal midbrain. Areas surrounded by a dotted box are presented at a higher magnification in the small panels at the right. Scale bar: 300 μm. (**B**) Experimental design for *in utero* electroporation and analyses using Cre-*loxP*-based neuron labeling in C. (**C**) Verification of mKO2-F-expressing cells using the proliferative marker Ki67. Cells expressing mKO2-F (magenta) were Ki67-negative (white), suggesting that NeuroD-promotor-driven mKO2-F expression is specific to post-mitotic cells. H2B-GFP (green) is expressed under the control of the CAG promotor. Larger pictures are stacked images. Scale bar: 100 μm. Areas surrounded by a dotted box are presented at a higher magnification in the small panels at the right. The images in the small panels are from a single plane. Yellow arrowheads indicate mKO2-F-positive neurons that are not labeled by the anti-Ki67 antibody. Green arrowheads indicate H2B-GFP-positive cells that co-express Ki67. Scale bar: 50 μm.

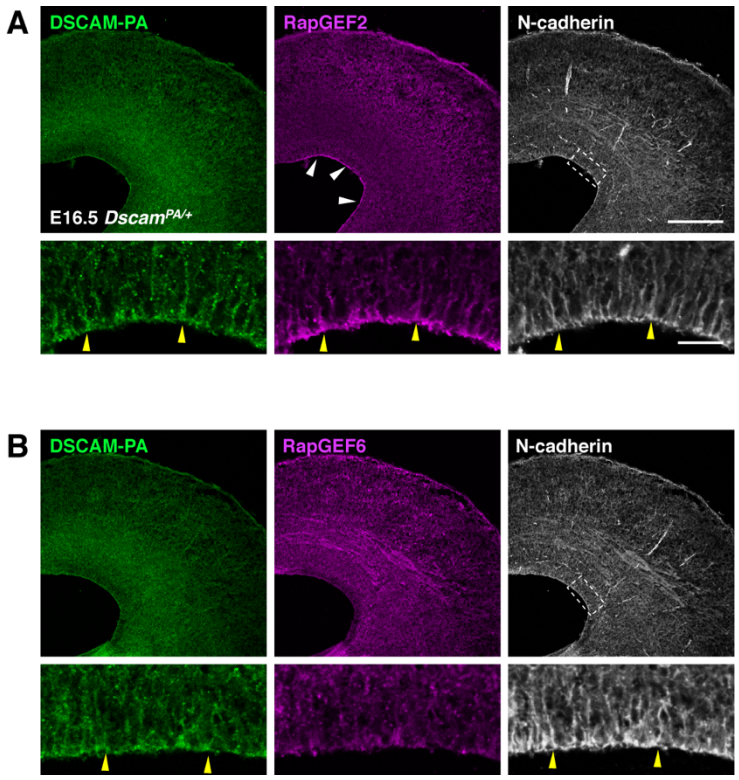

Fig. S7. Expression of RapGEF2 and RapGEF6 in the dorsal midbrain. Immunohistochemical staining for RapGEF2 (**A,** also shown in **Figure 4D**) and RapGEF6 (**B**) in the midbrain of E16.5 *Dscam*$^{PA/+}$ mice. (**A**) RapGEF2 localization was prominent at the ventricular surface (white arrowheads). Scale bar: 200 μm. (bottom) Higher-magnification image of the area enclosed in a dotted rectangle in the upper-right panel. Yellow arrowheads indicate radial fibrous staining. Scale bar: 20 μm. (**B**) RapGEF6 was not localized at the ventricular surface.

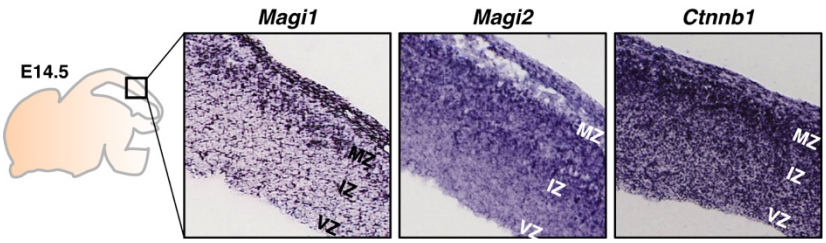

Fig. S8. Expression of *MAGI1, MAGI2,* and *β-catenin* transcripts. *In situ* hybridization analysis of an E14.5 mouse embryo (GenePaint.org) revealing the expression of *MAGI1, MAGI2,* and *β-catenin* transcripts throughout the dorsal midbrain in cells in the IZ, in which many post-mitotic neurons are localized. Several cells in the VZ are labeled with the probe (black arrows in enlarged image 3).

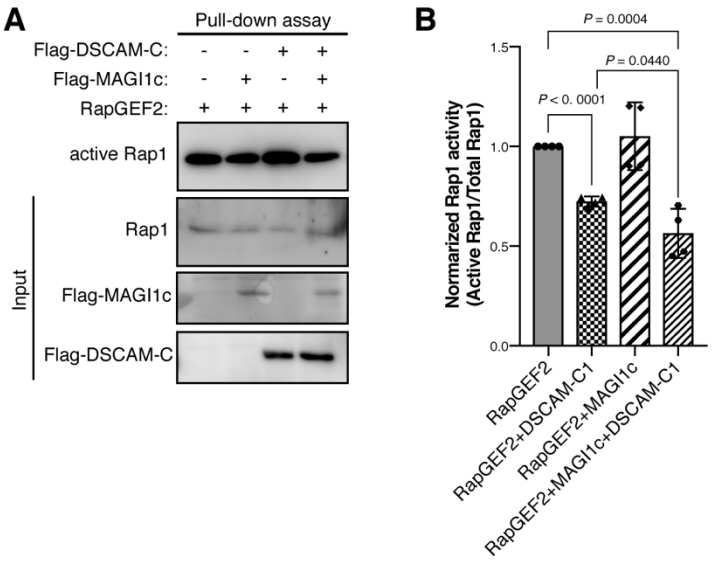

Fig. S9. Effect of MAGI1c on DSCAM-mediated suppression of RapGEF2 activity. (A, B) Pull-down assay evaluating active Rap1 in COS7 cells transfected with the indicated expression vectors. (**A**) The input (bottom three columns: 5%) and immunoprecipitants (upper column) were analyzed via western blotting using anti-Rap1 and anti-Flag antibodies. (**B**) Quantification of fold-changes of normalized Rap1 activities (active Rap1/total Rap1). Data are presented as the mean ± SEM values of four independent experiments; unpaired two-tailed *t*-test.

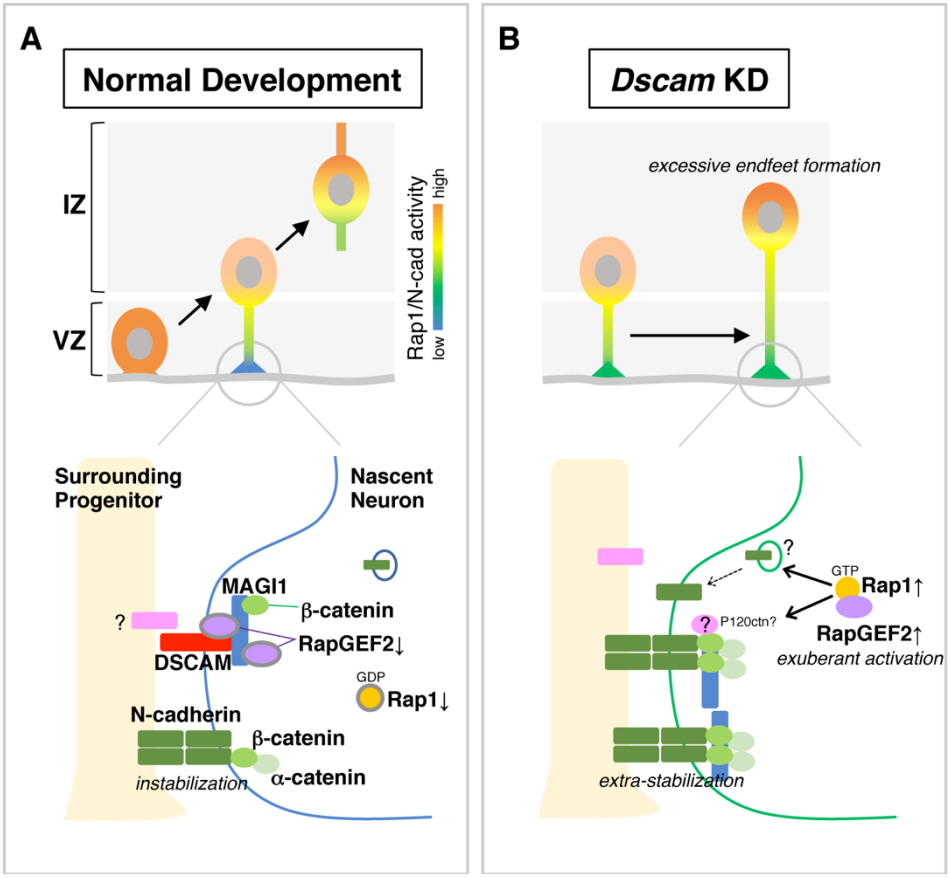

Fig. S10. Proposed model of the molecular mechanism of neuronal delamination. (**A**) Normally, expression levels of cadherin family members are relatively high in progenitor cells. To delaminate from the ventricular surface, N-cadherin-mediated AJs must be downregulated, especially at the apex of the endfeet with the palm-like structure abutting the ventricular surface. In nascent neurons, DSCAM is expressed upon neuronal differentiation and localizes at the endfeet apex. The cytoplasmic domain of DSCAM associates with and inactivates RapGEF2, forming a protein complex with MAGI1 and β-catenin. The spontaneous activity of Rap1 in cell adhesion is suppressed by the interaction of DSCAM with RapGEF2 or through the formation of the DSCAM/RapGEF2/MAGI1/β-catenin complex, causing instability of N-cadherin and AJs, concurrent with the attenuation of cadherin molecules by transcription factors. (**B**) When DSCAM expression is perturbed, nascent neurons can neither retract endfeet nor delaminate from the ventricular surface. In the absence of DSCAM, cell-intrinsic RapGEF2 and Rap1 activities are enhanced and promote N-cadherin-mediated AJ,

possibly through the regulation of p120ctn, the effector molecule afadin, or endocytosis, even though the transcriptional suppression of N-cadherin occurs. Finally, excess AJs suppress endfeet retraction and neuronal migration.

Section S1. Sequence of the NeuroD promotor (5'-3').

GAGCTCGGAGGACACTTGCTGGGAGCCTTGGTGTTTGTAACTCCGACTTGGAATCAAGG

CCACATTAGAATGCAGCAAAGCATGAACATTCAGGAAAGAGAGATCTTACTTCAAGTTC

CGGGAATATCCAGGTGTAGCTTTTCTTTTCAAAACTCCCTGGTCCGTTAGTCAGATCCCC

TGAGCCATAACTTCCACCGCTCCCCAATAACTCTCCTGTAGCATCCCCTAAAATGGAGA

GGTGAGAGCCAGAATCCGAGTTACATTTCACTGAATGAGGATATGCCAACTCTTCATAG

AAGGGCTGTCCCAATAAAATCTGCCTCTACTGTGCTTAACCTTCAAGATTTTTCTGCGGA

TCCAGGTATTTAAACGCAACACCCAGAGTAAATGAAAAAAAACAAAAACAAAACAAAA

AAACAACCCCCCCCCCCAAAAAAAAAGACAATGCTCCTTGCTTGCTCTGCTCTCAGCCA

GTTGACAGAACAAAGAAAAAGAAAAACTCCAGGCAGTTTATCTCTAGAATCCCAGAAT

GATTGGTGCCATGTTTTAGGCCACCAAAGAACTCCCACAATGCCTTGCTTTTCTTTTTAG

ATTCGTTCCGGGTCTGGAAGGTTACTTTCAATATCTTGCAAATGCCCAGGATCTCCTTAG

AACCCTCTCCCCCTCCCCTTTCCCAGATGTACCCCATTCCAGCCACTCAACCCTGACACT

GTTTGCAAACTCAAGGGCAATTGCCTTTACATAAGCAATTCAAGTAGGATGCATTCATT

GCAAAGGGGTTGAAGAGGGTAAGAACTTAATGAAGAGTTAGAAGAGGAACTGGAAAG

AGAAAGGAGGCCAACCATTCCTCCTCCTCCTCTGTCACTTTTCTTGGGCTAGAAGGACG

GAGGATCATCCATCTGAAAGATTCCTCCTTCAGATGGAGAAAATAAAGACTCCTTATTT

AAGAATAGATAAGGCTATTCCACAATAGACTTTGCTTGACTCAAAACACAGAGTCCCCA

GAAAGGGAAACAGCACATTGAATAGAGTTTTATTGCAGCTTCTCTTTGAGCTTCTTCTGA

CCAAGGCCCCAGAGATTGAGCACTAGGGGCTCAAGGAAGGCTGTGATTGAATTATGGTC

TGTGTCAGAGATGAAATTCCCACCTCTGGTGCGGGGTTGTTTAATCTTAGCATTCCCTAG

ATGAGCTAGCTGAGGTCATTCATTACTCCAGGAGCATCTGAAAACCAACGGAGCCAAGG

TCTGCTGGCAAAAACTAGCTTTAGACACAAAATTCTAGGGTTTAGAGTTGAAGACTCTT

AGTGAAGTCTCTGGGGTAGGAGCAGGTGACCGTTAGGTTTACATTTGGAGTGTTCAAGT

GTAGGGTATGGAAGCTGACTTGCAAAGGATTCTAGAAGATGCTCTAGTCAGGAAGGTTG

AGTCAAGGCTGTGTTTCCAGATGAGGTCGTTTTTATATGAAATAAATGTTTGCCTAGAGA

GGTGATGGAGATTAGAAGCCAGCCACCCTTTGGTGGCAATAAGCAAAGCCTCTGCTAAG

AGGTAGAAGCTAAGAGATGGGCCTCTCCAGAGAGAACAAAGTCAAACTGCACCACCGG

AGACCATTGTCAAGGGAAGGACCCTTCAGTGCACCTCAGTATCTGGGATTGTGAGTGGT

TCACCTCTGTCTACCTCTCTGCGCTAAAGCAGTCTTCAGGCTAGGACATAGACTCAGTGA

TCTTTCTTTACCTTTCCAGCTCGCCTCCCGCAACCCCCCCCCCCCCCACATGTCCTCTGTC

TTCTGCTGCCACAAAGGGTTAATCTCTCCTGCGGGTAAAAACAGGTCCGCGGAGTCTCT

AACTGGCGACAGATGGGCCACTTTCTTCTGGCCACAAAGGGGCCGGAATGGAGCGCTCC

GCGGCATACAAATAGGCAGGTCACGTGGTTCCCGGCTCTTGGCTGGACCGGGAAGACCA

TATGGCGCATGCCGGGGAGGAAGGAGCAGGGGCGGAGGTACTGTGGGGGTGAGGGGA

GTGGTGGTGGAAGGGGGCGGGAGGAAAGTTCTGGGGAGGGGTGAATGAGGGCGGGAG

TCGTTCAGTCTGGACGCGTGCGCGATTGCGGGGCGCAGGGACCTGCTCGTTGCTCAGCT

CACGGCCCCGCCCGCGCTCAGCATCAGCAACTCGGCTATATAACCCTAGCGCCCGCGCC

ACCGGGACACGAGGAATTC

Additional files

Movie S1. Neuronal delamination of a control neuron from the ventricular surface.

Movie S2. Excessive formation endfeet of *Dscam* KD neuron.

Supplementary table S1: List of DSCAM-interacting molecules identified using mass spectrometry.